# Inherent envelope fluctuations in forward masking: Effects of age and hearing loss.

Marc A. Brennan[1], Adam Svec[2], Afagh Farhadi[3], Braden Maxwell[3], & Laurel H. Carney[3]

[1]University of Nebraska-Lincoln, Lincoln, NE 68583

[2]San José State University, San Jose, CA 95192

[3]University of Rochester, Rochester, NY 14642

Correspondence:

Marc Brennan

University of Nebraska-Lincoln

4075 East Campus Loop

Lincoln, NE 68583

Fax: 402 472 3814

Phone: 402 472 3079

Email: Marc.Brennan@unl.edu

ABSTRACT

Forward masking is generally greater for Gaussian noise (GN) than for low-fluctuation noise (LFN) maskers for listeners with and without sensorineural hearing loss (SNHL). Because older age and SNHL may affect recovery from masker envelope fluctuations differently, the current study explored which of these two factors contributed more substantially to the persistence of GN disruption. GN disruption was measured using three masker-signal delays (25, 75, and 150 ms) for three adult participant groups: younger listeners with normal hearing (YNH), older participants with normal, or near-normal, hearing (ONH), and older participants with sensorineural hearing loss (OSNHL). The role of underlying mechanisms was tested using a computational model for midbrain neurons. The primary result suggests that older listeners with normal or near normal hearing may be more susceptible to the deleterious effects of masker-envelope fluctuations than younger listeners with normal hearing. Results from the computational model propose that there may be a larger influence of efferent feedback and saturation of inner hair cells on GN disruption than previously expected.

**Keywords:** aging, hearing loss, forward masking, auditory model

**Abbreviations:** Auditory Nerve (AN), Auditory Nerve Fiber (ANF), Gaussian noise (GN), inferior colliculus (IC), inner hair cell (IHC), low-fluctuation noise (LFN), low/high-spontaneous rate (L/HSR), Medial Olivocochlear (MOC), normal hearing (NH), outer hair cell (OHC), older participants with normal, or near-normal, hearing (ONH), older participants with sensorineural hearing loss (OSNHL), sensorineural hearing loss (SNHL), younger participants with normal hearing (YNH).

# I. INTRODUCTION

The temporal envelope of Gaussian noise (GN) contains short-term fluctuations in level. As the bandwidth of GN decreases, these fluctuations tend to increase the amount of masking for both simultaneous maskers (Pumplin, 1985; Zurek and Durlach, 1987; Hartmann and Pumplin, 1988; Kohlrausch *et al.*, 1997; Savel and Bacon, 2003) and forward maskers (Moore, 1981; Svec *et al.*, 2015, 2016) relative to a masker of equivalent bandwidth and level, for which the temporal envelope fluctuations have been minimized, referred to here as low-fluctuation noise (LFN). Given that less forward masking is generally expected and observed for LFN than for GN (e.g., Svec *et al.*, 2015, 2016), the additional masking attributed to the envelope fluctuations is often assessed by subtracting the LFN threshold from the GN threshold, referred to here as GN disruption. Considering that masker fluctuations contribute negatively to speech recognition (Stone *et al.*, 2011, 2012), identifying the mechanisms that contribute to GN disruption has implications for understanding the processes that contribute to speech recognition difficulties often experienced by older people with normal, or near-normal, hearing (ONH) and with sensorineural hearing loss (OSNHL; Füllgrabe *et al.*, 2015; Brennan *et al.,* 2016). The purpose of this study was to ascertain plausible mechanisms that contribute to GN disruption as a function of age and hearing status. To accomplish this, GN disruption was assessed in younger and older participants with NH, as well as older participants with SNHL, at masker-signal delays extending to near the presumed time constant of recovery from forward masking (Jesteadt *et al.,* 1982).

## A. Cochlear Compression and Listener Uncertainty

Forward masking is thought to reflect cochlear compression. For forward masking tasks, both Oxenham and Moore (1997) and Derleth *et al.* (2001) asserted that the effects of recovery

from forward masking for listeners with SNHL can be modeled by simply introducing a loss of cochlear compression, and thus greater responses to the masker in these listeners, resulting in shallower slopes of recovery for listeners with SNHL relative to listeners with NH. For these modeling approaches, the time constant of recovery, or the earliest masker-signal delay that results in masked thresholds matching quiet thresholds, was not assumed to be affected by the loss of cochlear compression. Under these assumptions, the time constant of recovery for forward masking should be independent of hearing status, and listeners with NH and SNHL should both entirely recover from forward masking and return to near quiet thresholds by 150-300 ms, the duration for which listeners have typically recovered from forward masking (e.g., Jesteadt *et al.*, 1982). While that may be a safe assumption for certain forward-masking conditions, the time course for recovery from GN disruption appears to be longer in duration for listeners with SNHL than for listeners with NH, which led investigators to speculate that some mechanism other than cochlear compression alone may contribute to the differences for GN disruption between listeners with NH and SNHL at longer masker-signal delays (Svec *et al.*, 2016).

Possible explanations might include that the persistence of listener uncertainty is longer for listeners with SNHL than for listeners with NH. For listeners with SNHL, a linearized cochlear response should yield larger amplitude peaks than a compressive cochlear response (NH), which would likely yield greater GN disruption. These larger amplitude peaks may result in the increased potential for confusing an amplitude fluctuation near the end of the masker duration for the onset of the brief signal, referred to as either listener uncertainty or the "confusion effect" (Neff, 1986). For listeners with NH, confusion between a narrowband masker and a sinusoidal target that are separated by brief masker-signal delays (< 20 ms) has been reduced by additionally presenting a copy of the masker in the contralateral ear. The diotic presentation effectively centers the auditory image of the masker in the listener's head, while the percept of the target remains in the test ear

(Neff, 1986). The results of Svec *et al.* (2016) revealed that the binaural cue from a diotic forward masker elicited a reduction in GN disruption at a masker-signal delay of 75 ms for listeners with SNHL. In that study, however, approximately half of the GN disruption was still observed for listeners with SNHL after presenting a binaural cue, suggesting that controlling for listener uncertainty did not account entirely for the magnitude of GN disruption for listeners with SNHL.

B. Inhibition at the Inferior Colliculus

Multiple peripheral and central processes, such as the middle-ear muscle reflex, neural adaptation, efferent innervation associated with the medial olivocochlear bundle, and dynamic range adaptation among neurons at multiple stages of the auditory pathways could also contribute to forward masking and, by extension, to GN disruption (See a review by Jennings, 2021). Nelson *et al.* (2009) argued that single auditory-nerve fibers (ANFs) tuned to the frequency of the target signal cannot account for forward masking due to a limited dynamic range of discharge rates and maximum threshold shifts, two attributes of ANF responses (in anesthetized animals) that do not mirror psychophysical forward-masking results. After measuring recovery from forward masking at the level of the inferior colliculus (IC) in awake marmosets, Nelson and colleagues asserted that the phenomenon of forward masking is less likely a consequence of excitation associated with the masker temporally overlapping with the target (e.g., “masker persistence”, as suggested by DiGiovanni *et al.*, 2018), but rather an increase in inhibitory responses for neural networks between the auditory nerve and the IC. This inhibition was hypothesized to arise from superior paraolivary nuclei projections to the IC (Nelson *et al.,* 2009; Gai, 2016; Salimi *et al.* 2017). Faure *et al.* (2003) argued that forward masking occurs because of a network of neural inhibition associated with the masker offset that impacts the internal representation of the target. While it remains unclear whether these inhibitory responses are expected to differ between GN and LFN,

recent work in physiology has suggested that GN disruption is observable from extracellular recordings of IC cells in awake rabbits (Fan *et al.*, 2021).

C. Medial Olivocochlear Efferent System

The Medial Olivocochlear (MOC) efferent system could play a role in GN disruption. The MOC provides efferent input to the outer hair cells (OHCs) that regulates OHC electromotility. Increased rate from the MOC is associated with decreased OHC electromotility and, in turn, reduced cochlear gain and smaller vibrations on the basilar membrane (Fuchs and Lauer, 2019). Upward rate-level shifts of 2-14 dB for the auditory nerve with electrical stimulation of the MOC have been observed (Gifford and Guinan, 1983), with the largest shifts occurring between 45-75 dB SPL (Guinan, 2018). The MOC efferent system receives ascending inputs from peripheral auditory neurons, as well as descending projections from the IC and other more central auditory structures (Mulders and Robertson, 2000; Schofield, 2011). While the cumulative contribution of the MOC to auditory physiology and perception remains unclear (e.g., Jennings, 2021), Carney (2018) argued that one purpose of the MOC efferent pathway might be to regulate the saturation of inner hair cells (IHCs), thereby controlling low-frequency temporal fluctuations in ANF responses, referred to as neural fluctuations. Due to the fact that IC neurons are sensitive to envelope fluctuations (reviewed in Joris *et al.,* 2004) and the IC includes descending projections to the MOC, Carney additionally argued that neural fluctuations may excite MOC efferents and decrease OHC electromotility, leading to reduced cochlear gain. Farhadi *et al.* (2021) modeled IC firing rate as a function of time in response to amplitude-modulated stimuli. Modeling results suggested that predictions were not accurate without the inclusion of efferent-regulated cochlear gain driven by IC inputs to the MOC system, providing additional support for the assertion that fluctuating inputs to the IC are likely directly impacting MOC spike rates, and in turn, cochlear

gain. The effect of this decreased cochlear gain in response to a fluctuating input, such as GN, should be decreased IHC saturation, and thus greater ANF fluctuations. In contrast, a minimally fluctuating input, such as LFN, should lead to reduced ANF fluctuations relative to GN.

The time course of decreased cochlear gain following stimulus presentation begins to decay within 25 ms of the masker offset (Roverud and Strickland, 2010), but appears to remain, in diminished form, up to 75 seconds following stimulus presentation (Brown, 2001; Cooper and Guinan, 2003). This initial time course of decreased cochlear gain following stimulus presentation shares correspondence with the time course of recovery for forward masking, with an exponential decay in masking that extends from 0 to approximately 128 ms following masker offset (e.g., Jesteadt *et al.,* 1982). If cochlear gain is influenced by temporal-envelope fluctuations through IC projections to the MOC, masker envelope fluctuations associated with a GN forward masker should induce a reduction in cochlear gain and a concomitant decrease in the response of the IC to a target stimulus that temporally follows a masker stimulus. Consequently, the time course of recovery from forward-masker envelope fluctuations (e.g., the duration between masker offset and return to quiet threshold) would be expected to follow the known time course of decreased cochlear gain following stimulus presentation, primarily from 25 to 125 ms (Brown, 2001; Cooper and Guinan, 2003; Roverud and Strickland, 2010; Rabbitt and Brownell, 2011). In contrast, when the IC is presented with relatively few temporal-envelope fluctuations (e.g., LFN), the IC projections to the MOC should induce less cochlear gain reduction relative to a stimulus with more robust fluctuations (e.g., GN). The potential net effects would likely result in a lower IC rate in response to a target following a LFN forward masker than for a GN forward masker, which is consistent with GN disruption. These effects of the MOC efferent system could conceptually account for the gradual decrease in GN disruption observed as a function of increasing masker-signal delays (25, 50, and 75 ms) for participants with NH (Svec *et al.,* 2016).

Additional important factors moderating the MOC influence on GN disruption are: a) the *relative* degree of IHC saturation in response to the GN and LFN forward maskers; and b) changes in MOC physiology associated with age and SNHL. As described above, IHC saturation determines the neural fluctuations in response to these two types of maskers. The relative IHC saturation in response to these maskers, and thus the neural fluctuations and the MOC responses that they elicit, would be expected to vary across groups of listeners. For younger listeners with audiometric thresholds within normal limits, IHCs will tend to saturate in response to both GN and LFN forward maskers when presented at high sound levels, resulting in a relatively small amount of predicted GN disruption for moderate and high-level maskers. For older listeners with slightly elevated audiometric thresholds (e.g., small amounts of hearing loss), less IHC saturation would be expected. Although older listeners have a less robust MOC efferent system (Yalcinkaya *et al.,* 2009), neural fluctuations and changes in cochlear gain would still be expected, which together may result in relatively large GN disruption for older listeners with small amounts of hearing loss. For listeners with significant SNHL, two factors may impact the magnitude of observed GN disruption. First, even when masker presentation levels are high, IHCs might not saturate for either GN or LFN maskers due to threshold elevation. Second, the impact of the MOC efferent system on cochlear gain is reduced as a consequence of the gain reduction associated with SNHL (Carney, 2018; Fuchs and Lauer, 2019). Consequently, less GN disruption would be expected for older listeners with substantial SNHL than for older listeners with minimal hearing loss. After an initial cochlear-gain decrease associated with an input stimulus, an intact MOC system allows cochlear gain to increase during the interval from 25 to 125 ms or more after stimulus offset (Brown, 2001; Roverud and Strickland, 2010), implying that differences in GN disruption for younger listeners with normal hearing (YNH), ONH, and OSNHL should be maximal at a short masker-signal delay and dissipate with longer masker-signal delays.

## D. Physiologically-Inspired Computational Models

To date, computational models of the auditory system have not been used to clarify possible physiological mechanisms associated with GN disruption. However, computational models have been used extensively to examine mechanisms associated with forward masking (Dau *et al.*, 1996; Derleth *et al.*, 2001; Meddis and O'Mard, 2005; Nelson and Young, 2010; Gai, 2016; Salimi *et al.*, 2017). The auditory models used thus far have included various properties of the auditory system, including the compressive nonlinearity, filtering of the cochlea, adaptation of the auditory nerve, and modulation filtering within the central auditory system (e.g., Derleth *et al.*, 2001). Only a subset of these models included the stochastic firing, onset response, and saturation response properties of the auditory system (Meddis and O'Mard, 2005; Nelson and Young, 2010; Gai, 2016; Salimi *et al.*, 2017). While Meddis and O'Mard (2005), Nelson and Young (2010), Gai (2016), and Salimi *et al.* (2017) attempted to model properties of the IC, only Meddis and O'Mard attempted to predict behavioral performance. In contrast, Salimi and colleagues attempted to model rate-level functions for growth of masking. While the previously mentioned computational models did not include the efferent system, the potential influence of the MOC efferent system on auditory perception has been successfully examined using computational models for simultaneous masking with broadband GN (Jennings *et al.,* 2011). Clearly, additional computational modeling work is needed to understand the entirety of the mechanisms contributing to GN disruption.

Other attempts to relate the MOC physiological response to behavioral effects have involved comparing conditions assumed to invoke the MOC system to conditions less likely to invoke the MOC system (e.g., Wojtczak *et al.,* 2019), examining psychophysical measures in animals or humans lacking an MOC efferent system (Sharf *et al.*, 1997; Smith *et al.*, 2000), or—as noted above—attempting to account for behavioral thresholds using computational models that

include the efferent system (Winslow and Sachs, 1988; Jennings *et al.,* 2011). For a comprehensive review of the potential effects of the MOC system on behavior, see Jennings (2021). Establishing a definitive relationship of MOC function to behavioral effects has been difficult, despite at least 30 years of investigation (e.g., Winslow and Sachs, 1988; Jennings *et al.,* 2011; Wojtczak *et al.,* 2019). Reasons for the discrepant results are unclear, but contributing factors may include normal variance in otoacoustic emissions limiting its ability to accurately assess MOC function, non-peripheral masking, and, among other potential reasons, type of stimuli tested (Jennings, 2021). The approach adopted for this experiment was an attempt to determine whether a computational model that includes the physiological response of the MOC efferent system and the IC could account for GN disruption.

## E. Research Questions

To clarify possible physiological mechanisms associated with GN disruption, the current study examined the effects of age and SNHL on forward-masked thresholds when presented with maskers that either did (GN) or did not (LFN) rapidly fluctuate in level over time. Masked thresholds were obtained for a 4000-Hz pure-tone signal when presented after the offset of GN or LFN maskers at three different masker-signal delays (25, 75, and 150 ms) for YNH, ONH, and OSNHL participants. The following hypotheses were formed:

1) If cochlear compression strongly contributes to GN disruption, then—due to the loss of cochlear compression—GN disruption should be greatest for the OSNHL participants, followed by the ONH and YNH participants.
2) If differences in the physiological response of the MOC efferent system for GN and LFN maskers strongly contributes to GN disruption, then GN disruption should vary non-monotonically with audiometric threshold at the target frequency. The largest effect is

hypothesized to occur for listeners with relatively small amounts of hearing loss (e.g., ONH participants), for whom IHC saturation and neural fluctuations would differ the most between the two masker types.

For all mechanisms that contribute to GN disruption, differences in GN disruption by group were hypothesized to decrease as the masker-signal delay increased.

## II. METHODS

### A. Participants

A total of 57 participants were enrolled in this study. Five participants were excluded because they did not qualify on the basis of their hearing thresholds (see below). Of the remaining individuals, 18 YNH (19 – 25 years, M=22), 14 ONH (65 – 81 years, M=71), and 20 OSNHL (62 – 82 years, M=71) participants completed the study. Within each participant group, the age of the participants was evenly distributed across their respective age ranges. A graduate student in audiology measured hearing thresholds (ANSI, 2004) for all participants using conventional audiometry (ASHA, 2005) at 6000 Hz and at octave frequencies from 250 to 8000 Hz. Hearing thresholds for the test ear are plotted in Fig. 1. Hearing thresholds for the non-test ear were within 15 dB of the test ear as measured by pure tone average (500, 1000, 2000 Hz). NH was defined as hearing thresholds less than 30 dB HL from 250 to 4000 Hz. However, one ONH participant with a hearing threshold of 30 dB HL at 500 Hz participated. SNHL was defined as air conduction thresholds from 35 to 65 dB HL at 4000 Hz and, for frequencies with hearing loss greater than 25 dB HL, bone conduction thresholds within 10 dB of the air conduction threshold. Participants who did not have NH, SNHL outside the range of 35 to 65 dB HL at 4000 Hz, or a 25 dB or greater difference in air-conduction thresholds between the two ears at 4000 Hz did not qualify. All subjects were native English speakers. Data were collected at University of Nebraska-Lincoln.

Approval for this study was obtained from the Institutional Review Board. Participants consented to join the study and were reimbursed monetarily for their time.

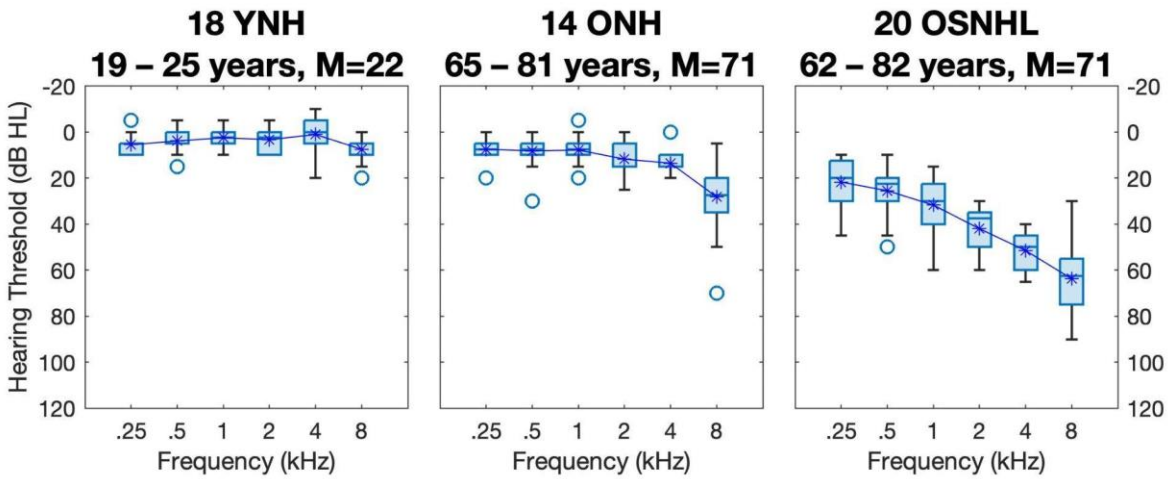


Fig. 1. (color online) Plots of hearing threshold for each participant group. Number of participants, age range, and median age are also provided. For this and the remaining box and whisker plot, each box represents the interquartile range, each line represents the median, each asterisk represents the mean, each circle represents an outlier (>1.5 times the interquartile range), and whiskers represent the most extreme value that is not an outlier.

B. Stimuli and Apparatus

Stimuli were generated using a personal computer (22.05 kHz sampling rate; 16 bits per sample) and custom MATLAB (2019a) scripts. The masker was either GN or LFN, each with one-third equivalent rectangular bandwidth (1/3 $ERB_N$) centered at 4000 Hz. Maskers were 400 ms in duration with 5-ms cosine-squared ramps. LFN was generated using a Hilbert transform (Buss *et al.,* 2006) with the PsyAcoustX package (Bidelman *et al.*, 2015). Specifically, the Hilbert envelope was computed for each 1/3 $ERB_N$ GN generated. Each GN was divided in the time domain by its

Hilbert envelope and then multiplied by the original spectral region in the frequency domain; these last two steps were completed ten times to yield the final version of LFN.

The signal was a 4000-Hz pure tone, 10 ms in duration with 5-ms cosine-squared ramps. The signal was presented either without the masker (quiet condition) or with the signal onset 25, 75, or 150 ms after the masker offset (masker conditions). All durations were measured from the 0-amplitude points of the onset and offset ramps. Stimuli were calibrated using a 6-cc flat plate coupler and a Larson Davis System 824 sound level meter (Depew, New York). Signal levels are reported as the root-mean-square peak equivalent (0.707 x peak pressure) in dB SPL. These 24-bit digital stimuli were then converted to analog (RME Babyface sound card, Haimhausen, Germany), amplified by a HeadAmp 4 Pro headphone distribution amplifier (Baton Rouge, Louisiana), and presented to one ear using Sennheiser HD-25 headphones (Wedemark, Germany). All testing took place in a single-walled sound attenuated room, with each participant sitting in front of a touch-screen monitor.

## C. Procedures

For all experimental conditions, the signal level was varied adaptively to estimate threshold corresponding to 71% correct with a two-down, one-up rule (Levitt, 1971). For all masker conditions, the masker level was fixed at 80 dB SPL. To ensure audibility of the signal for the OSNHL participants, the starting level for the signal was 80 dB SPL. Initial step size was 18 dB, reducing to 9 dB after the first reversal and 6 dB after the second reversal. The remaining step size was 3 dB. Data collection ended after a total of nine reversals. The minimum signal presentation level was -10 dB SPL, and the maximum signal presentation level was 90 dB SPL. Thresholds for tracks with three presentation levels in a row at 90 dB SPL were recorded as 93 dB SPL. Otherwise, the average of levels at the last four reversals was taken as a threshold.

A trial consisted of three observation intervals separated by 300 ms. Each interval was marked by a separate button which was illuminated on the touchscreen monitor for approximately 1200 ms. For the absolute-threshold condition, one randomly-selected interval contained the signal. For the masker conditions, one randomly-selected interval contained the masker and signal, the other two contained only the masker. Participants indicated the interval which they believed contained the signal by pressing the corresponding button and feedback was provided. For each condition, threshold was measured three times and the final threshold was recorded as the average across the three measurements. Threshold for the absolute-threshold condition was measured first followed by the masker conditions in random order.

D. Computational Model

A computational model for auditory nerve (AN) and midbrain fiber responses (Nelson and Carney, 2004; Zilany *et al.,* 2009, 2014; Farhadi *et al.*, 2021), with peripheral tuning for human listeners (Ibrahim and Bruce, 2010), was used to provide insight into possible mechanisms that contribute to GN disruption. Figures 2 and 3 provide overviews of the computational model. Firing rates (described below) are depicted for one trial of each masker type for someone with a hearing level threshold of 15 dB at 4 kHz (i.e., an ONH listener). One issue to resolve is the selection of characteristic frequencies (CFs) to include. Presumably, listeners are using CFs tuned near the target and masker center frequency of 4 kHz. Due to filtering of masker frequency components, ANFs tuned to a masker edge frequency will have larger fluctuations (for both masker types) than ANFs tuned to the masker center frequency. For the same reason, there will be less IHC saturation and responsiveness to the target stimulus. Here it was assumed that listeners integrated firing rates for fibers tuned to CFs that extended slightly beyond the bandwidth of the masker (3.9-4.1 kHz).

Specifically, for each stage of the model, the characteristic frequencies (CFs) were 3.6, 3.7, 3.8, 4, 4.2, 4.3, and 4.5 kHz.

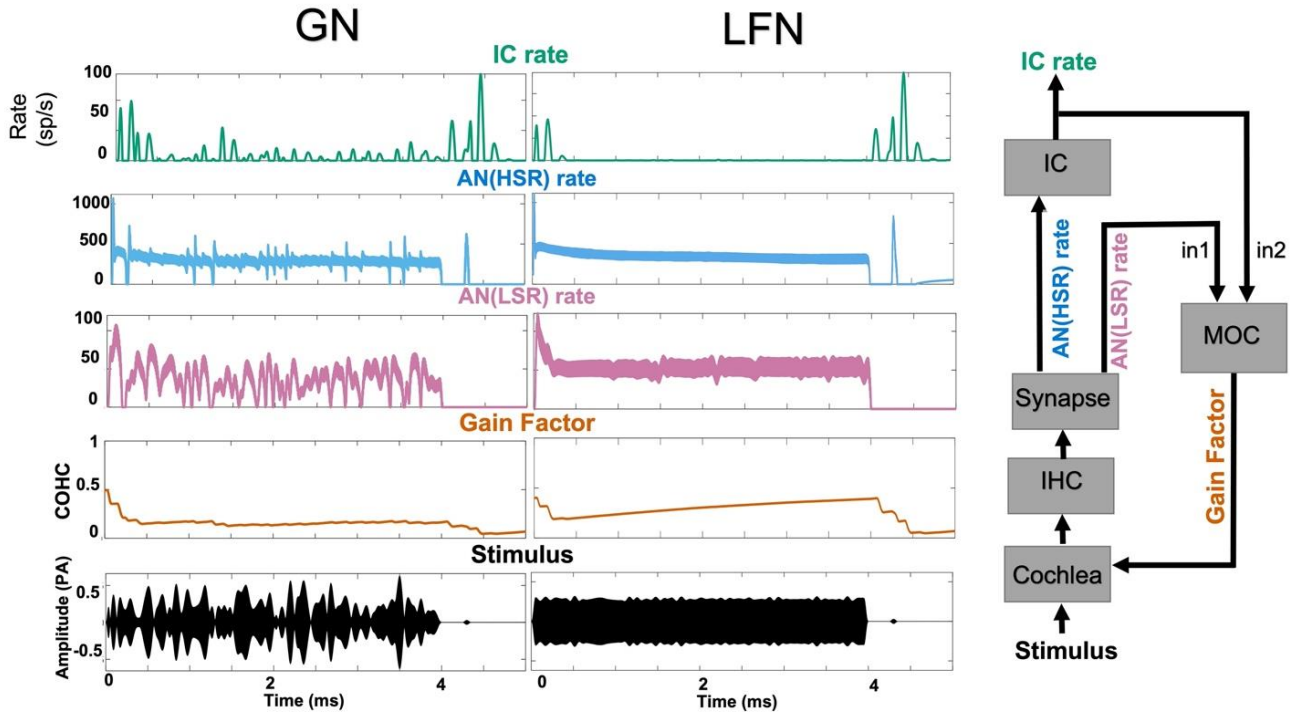


Fig. 2. (color online) Computational model with addition of MOC efferent system. **a)** Representations of targets with GN (left) and LFN (right) maskers for ONH with **b)** a LSR ANF, and **c)** HSR)ANF. ANF characteristic frequencies = 4 kHz **d)** Onset of masker reduced cochlear outer hair cell gain (COHC). Due to fluctuations in the representation of the GN masker, this reduction in COHC gain was maintained over time for the GN masker but not the LFN masker. **e)** This effect resulted in a more robust representation of the target with the LFN masker than the GN masker for the IC.

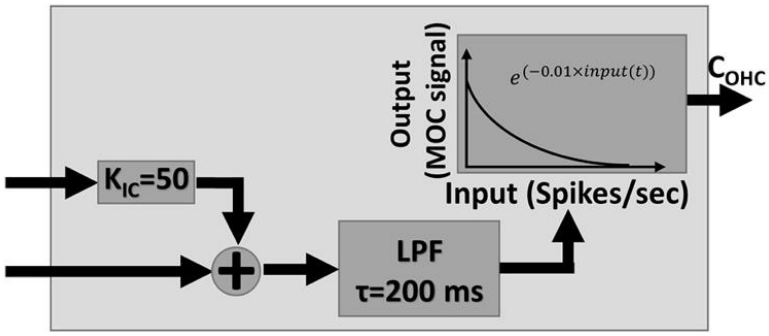


Fig. 3. Computational model of MOC efferent system. Depicts mapping of input spike rate to MOC gain factor to cochlea. Input spike rate from IC is scaled and added to that from a low-spontaneous rate auditory nerve fiber, low-pass filtered, and then converted to MOC gain factor. Higher MOC spike rate results in smaller gain factor.

The computational model incorporated the probabilistic rate functions of ANFs, as well as other properties, including IHC transduction and synaptic saturation and adaptation. The AN model includes lowpass filters corresponding to the outer and inner hair cells, each with adjustable scaling factors. Decreasing the OHC value (max=1, min=0) decreases cochlear gain, while decreasing the IHC value decreases sensitivity of the IHC and increases the dynamic range (i.e., pushes the saturation point of the IHC nonlinearity to higher input levels). The OHC and IHC scaling factors were set to match the mean audiometric threshold in dB HL for each participant group. Two-thirds of the threshold shift was ascribed to OHC, based on acoustic trauma observed in cats (Bruce *et al.,* 2003; Zilany and Bruce, 2007) and estimated OHC integrity in humans with SNHL (Plack *et al.,* 2004). Modeling of the AN consisted of implementations of low- and high-spontaneous rate fibers (LSR, HSR).

The LSR fibers provided the ascending neural input to the MOC, representing responses of cochlear nucleus neurons with wide dynamic ranges that receive inputs from low- and medium-spontaneous rate fibers and project to the MOC (Ye *et al*., 2000). The MOC model was based on

Farhadi *et al.* (2021). The HSR fibers provided input to the IC, which in turn provided the descending neural input to the MOC. The two inputs to the MOC stage of the model were scaled to approximately equalize firing rates (Figure 3). The MOC stage converted the input rates to a gain factor that modulated the cochlear gain. This conversion was an exponential relationship of firing rate to gain: the cochlear gain factor decreased exponentially as the combined input to the MOC stage increased. The final step in the MOC model stage was a low-pass filter with a time constant of 200 ms, which was chosen to approximate the overall time course of the MOC system. Because the model of the IC that provided input to the MOC feedback consisted of a best modulation frequency of 64 Hz), regulation of cochlear gain was driven by both overall stimulus level (via the AN LSR input) and envelope fluctuations (via the IC input).

As illustrated in Fig. 2d, cochlear gain decreased after masker onset (due to high firing rates at stimulus onset for both the IC and ANFs). For the GN masker, this initial reduction in OHC gain was maintained throughout the duration of the masker and, due to the sluggishness of the MOC system, for a period after the onset of the masker. For the LFN masker, this initial reduction in OHC gain was reduced over time (due to a reduction in firing rate from the IC). For the IC, these effects resulted in a more robust representation of the target with the LFN masker than with the GN masker (Fig. 2e). HSR ANF model responses from the AN model with efferent feedback (Fig. 2) provided inputs to same-frequency inhibitory-excitatory IC model cells (Carney and McDonough, 2019) with best modulation frequency of 64 Hz.

Model IC responses were obtained for a ~30 dB range of target levels near an initial, rough approximation of threshold with the model. Target levels were spaced 3 dB apart, and 50 trials were completed per target level. For each trial, the standard and target intervals were separated by 500 ms (order was balanced equally), and the model-IC instantaneous firing rate was recorded from 300 ms after masker onset until the end of the interval. After averaging across CFs, the

interval with the higher maximum instantaneous rate during this timeframe was selected as the target interval for that trial. From this, proportion correct was computed for each target level, and a logistic function was then fit to each performance-intensity curve. Threshold was estimated as the level for which the curve intersected the 70.7% correct point. As an initial attempt, this process was completed using the 25-ms masker-signal delay and repeated for each masker type and participant group.

### E. Analysis

All statistical models were computed using IBM SPSS version 27 or MATLAB (2021b) and the statistics and machine learning toolbox. Quiet conditions across participant groups (YNH, ONH, OSNHL) were analyzed using a repeated measures analysis of variance. Post-hoc comparisons were completed using pairwise comparisons with false discovery rate adjustments (Glickman *et al.*, 2014). To assess for differences in masked threshold by masker type (GN, LFN), masker-signal delay (25, 75, 150 ms), and hearing status (NH, SNHL), a linear-mixed effects model with random intercepts for each participant was conducted. Reference conditions were set to YNH, 25 ms masker-signal delay, and LFN. Using YNH as the reference group allowed for the determination of the effect of age and hearing status by comparing threshold for YNH to ONH (effect of age) and OSNHL (effect of hearing status and age). Using the 25-ms masker-signal delay and LFN as the reference conditions allowed for the determination of whether GN disruption decreased from 25 to 75 ms or from 25 to 150 ms.

## III. RESULTS

### A. Absolute Thresholds

Figure 4 depicts detection thresholds in dB SPL. As expected, absolute thresholds (see Fig. 4, 150 ms panel) were best for the YNH participants, followed by progressively poorer thresholds for the ONH and OSNHL participants ($df$ = 2,50, $F$ = 194.2, $p$<.001). Post-hoc testing revealed that thresholds in quiet were significantly different for each group. Specifically, detection thresholds were significantly higher for ONH ($p$<.001, M=31.1, SD=6.2) and OSNHL ($p$<.001, M=65.2, SD=9.0) participants than for YNH participants (M=21.3, SD=5.4). Detection thresholds were also significantly higher for OSNHL than for ONH participants ($p$<.001).

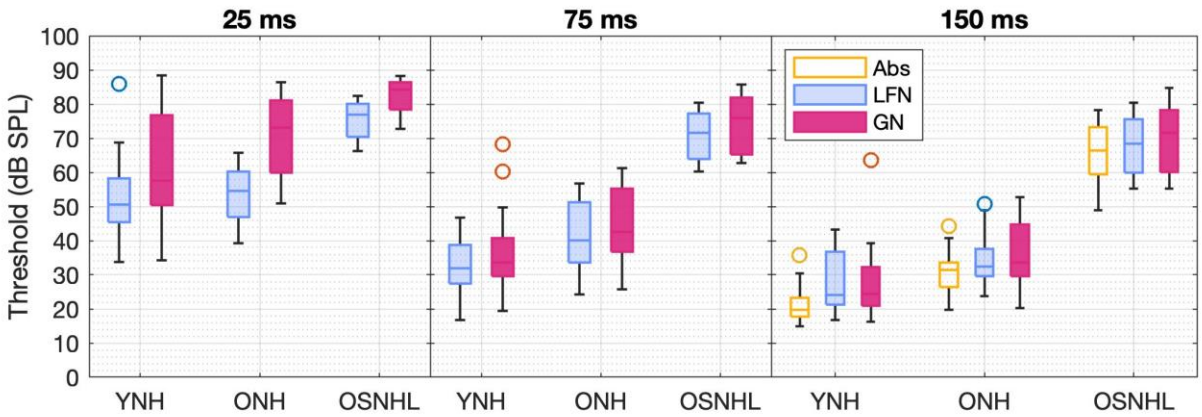


Fig. 4. (color online) Plots of threshold with the LFN and GN maskers for each delay time. Absolute (Abs) threshold shown for the 150 ms panel. Threshold decreased as delay time increased.

B. Masked Thresholds and GN Disruption

Consistent with prior work (Brennan *et al.,* 2015; Svec *et al.,* 2015, 2016) and as shown in Fig. 4, masked thresholds for all three masker-signal delays were lowest for YNH participants and then systematically higher for ONH and OSNHL participants. While not plotted, the amount of masking followed this same trend—specifically, was greatest for YNH and then systematically

less for ONH and OSNHL. For the LFN masker, thresholds for the 25-ms masker-signal delay time condition were significantly higher (poorer) by 23 dB for OSNHL than for YNH participants (t=7.5, $p$<.001) and did not differ significantly between ONH and YNH participants (t=1.3, $p$=.700).

As the investigators hypothesized, threshold for the 25-ms masker-signal delay was greater for GN than for LFN (i.e., GN disruption), as also shown in Fig. 5 and supported by the effect of the GN masker condition for the YNH participant group (8.5 dB, t=5.1, $p$<.001). Consistent with the second hypothesis regarding expected effects of IHC saturation on GN disruption, GN disruption for the 25-ms masker-signal delay time was significantly greater by 8.9 dB for the ONH participants than for the YNH participants (t=3.5, $p$<.001). In contrast, GN disruption did not differ significantly between the YNH participants and the OSNHL participants (-1.5 dB, t=-0.6, $p$=.519). For the 75-ms masker-signal delay, GN disruption was statistically equivalent to the 25-ms masker-signal delay (-4.0 dB, t=-1.7, $p$=.093) for the YNH participants. GN disruption then decreased significantly, by 8 dB, from the 25- to 150-ms masker-signal delay (t=-3.4, $p$<.001). The decrease in GN disruption from the 25- to the 75-ms masker-signal delay was significantly greater for the ONH than for the YNH participants by 10.2 dB (t=-2.9, $p$=.004). Similarly, the decrease in GN disruption from the 25- to 150-ms masker-signal delay was significantly greater for the ONH than for the YNH participants, by 7.3-dB (t=-2.1, $p$=.040). In contrast to the ONH participants, the decrease in GN disruption from the 25-ms masker-signal delay to the 75- and 150-ms masker-signal delays were statistically equivalent for the YNH and OSNHL participants (75 ms: 0.9 dB, t=0.3, $p$=.775; 150 ms: 2.9 dB, t=0.9, $p$=.379).

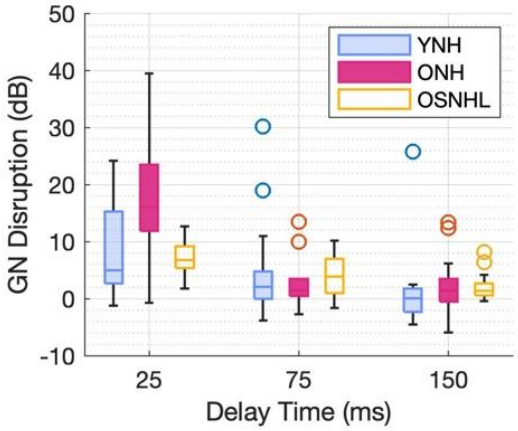


Fig. 5. (color online) Plot of GN disruption. For the 25-ms masker-target delay, GN disruption was larger for the ONH participants than for the other two participant groups.

In summary, GN disruption for the 25-ms masker-signal delay was significantly greater for ONH than for YNH and OSNHL participants. Recovery from GN disruption was greater (steeper) for ONH than for YNH participants, with similar GN disruption for the three participant groups for the two longest masker-signal delays.

C. Computational Model

Figure 6 plots OHC gain as a function of time for each masker and participant group. For all three groups and both masker types, OHC gain decreased following masker onset. For the computational model of YNH, OHC gain initially decreased due to an increase in the rate of the IC and LSR inputs to the MOC (see Fig. 2). Following this abrupt gain decrease, OHC gain gradually increased over the remaining duration of each masker. For the YNH group, the model proposes that these listeners would likely be operating in IHC saturation in the presence of a masker presented at 80 dB SPL. Due to IHC saturation, input fluctuations of the GN masker would be reduced, leading to a small difference between the masked thresholds for GN and LFN. The

reduction of masker envelope fluctuations at the level of the IC results in gradual OHC gain increase over the duration of each masker type. In contrast, for the computational model of ONH, the model proposes that these listeners would likely be operating below the saturation point of the IHC due to slight absolute threshold elevations, suggesting that robust envelope fluctuations from the GN masker would remain intact. This preservation of masker envelope fluctuations at the level of the IC results in gradual OHC gain decreases, as opposed to increases (YNH), over the duration of the GN masker. Consequently, there were larger differences in OHC gain, over time, between the two masker types (GN vs. LFN) for the ONH than for the YNH model. The OSNHL model proposes that the consequences of sensorineural hearing loss may lead to reduced OHC function, and therefore reduced ability to apply OHC gain increases or decreases, as well as reduced possibilities for IHC saturation. Consequently, smaller changes in predicted OHC gain were observed between the two masker types for this group.

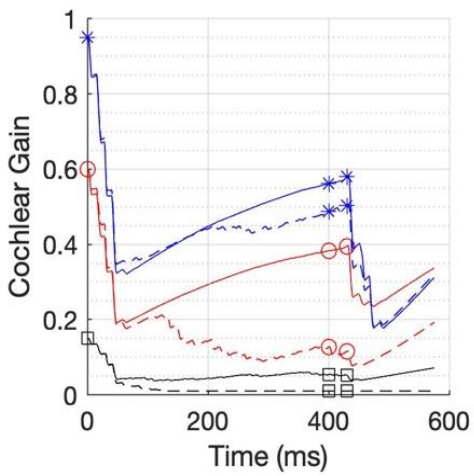


Fig. 6. (color online) Plot of OHC gain for masker-target delay of 25 ms. Responses are shown for one fiber with CF = 4.3 kHz. Differences in OHC gain between GN (dashed lines) and LFN (solid lines) were greater for ONH (circles/red) than for YNH (asterisks/blue) and OSNHL

(squares/black). Symbols denote, in temporal sequence, start of the masker, end of the masker, and temporal center of the 10-ms target.

Figure 7 illustrates the masked thresholds estimated from the computational model, with and without the efferent system. As predicted, masked thresholds with the efferent system were higher (poorer) than without the efferent system. The increase in thresholds for the LFN relative to the GN masker (i.e., GN disruption) were greater for the computational model when efferents were included rather than omitted. Note that the estimated thresholds were less than the behavioral thresholds, with this difference largest for the YNH group. Figure 8 shows GN disruption estimated by the computational model, as well as measured behaviorally. Without the efferent system, GN disruption was minimal for YNH and ONH. With the efferent system, the estimates of GN disruption for YNH and ONH increased by 3 and 18 dB, respectively, relative to the model without the efferent system. When the efferent system was included in the model, GN disruption was more similar in magnitude to the behaviorally measured GN disruption for all three participant groups. In addition, GN disruption estimated from the computational model with the efferent system was greatest for ONH.

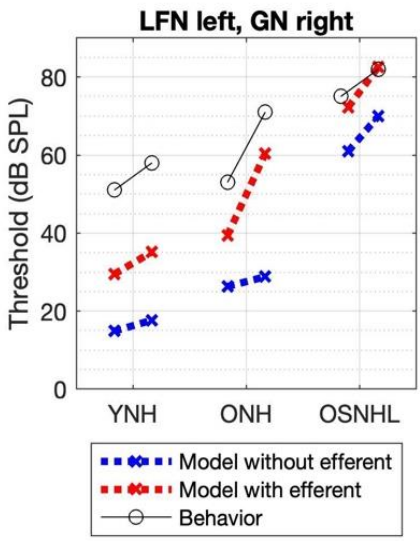


Fig. 7. (color online) Behavioral and model thresholds. Plots of mean behavioral and model predicted thresholds for YNH, ONH, and OSNHL with and without the efferent system (25-ms masker-target delay).

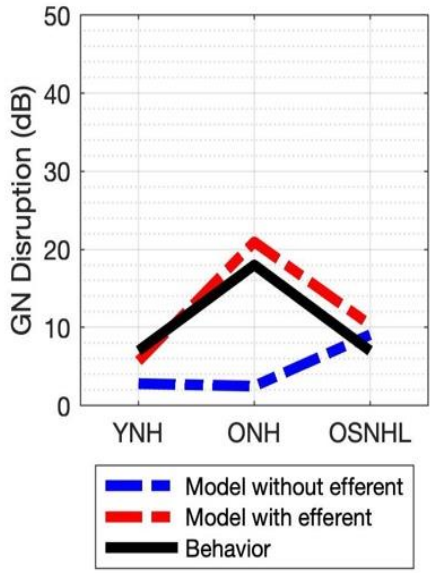

Fig. 8. (color online) Behavioral and model GN disruption. Plots of mean GN disruption for YNH, ONH, and OSNHL with and without the efferent system (25-ms masker-target delay).

## IV. DISCUSSION

### A. Primary findings

Factors proposed to contribute to GN disruption include cochlear compression, listener uncertainty, inhibition within the auditory system, and the MOC efferent system. Because cochlear compression, inhibition, and MOC function differ by age and hearing status, this study was designed to: a) examine the contributions of each mechanism to GN disruption by comparing GN disruption for young participants with NH to older participants with NH or SNHL; and b) examine the extent to which a computational model of the IC and MOC could account for the GN disruption observed in the behavioral results. The primary results suggest that older listeners may be more susceptible to the deleterious effects of masker envelope fluctuations, even in the absence of significant hearing loss, when compared to masked thresholds for younger listeners. Specifically, elevated GN disruption was observed for the 25-ms masker-signal delay for ONH participants relative to YNH and OSNHL participants. For all three groups, GN disruption was reduced for the two longer masker-signal delays (75, 150 ms), and at these longer delays, significant differences in GN disruption between the groups were no longer observed.

### B. Cochlear Compression

When subjected to the presentation of a GN masker, prior investigators have hypothesized that linearization of the basilar membrane associated with SNHL should result in greater amplitude for the peaks of masker envelope fluctuations, relative to a cochlea functioning normally (Svec *et*

*al.*, 2015). Consequently, the relative exaggeration of these fluctuations would likely cause increased difficulty for listeners with SNHL, relative to listeners with NH, when attempting to detect a target that temporally follows the masker (Svec *et al.*, 2016). Therefore, if cochlear compression strongly contributes to GN disruption, then GN disruption should have been greater in magnitude for the participants with SNHL than for the participants with NH. Instead, for the 25-ms masker-signal delay, GN disruption did not differ between the YNH and OSNHL participants and was *greatest* for the ONH participants. While not statistically significant, these same trends were present in the GN disruption data from Svec *et al.* (2015). These results, at face value, do not support the argument that variations in cochlear compression across individuals contribute toward differences in GN disruption. However, it is possible that GN disruption for the OSNHL participants was a consequence of a quasi-linearized basilar membrane response in the absence of MOC efferent feedback. This notion is supported by the estimated GN disruption for the computational model without MOC efferent feedback. For this model, greater GN disruption was predicted for the OSNHL participants (9 dB) than for the YNH and ONH participants (3 dB). This prediction of greater GN disruption for the OSNHL participants is consistent with a loss of OHC gain (and thereby compression) leading to larger fluctuations, and consequently, greater "modulation masking" by the GN masker. Note that these results in no way imply that larger GN disruption could not be observed for OSNHL relative to YNH or ONH (i.e., with the evaluation of different stimulus conditions than used here).

## C. Listener Uncertainty

The results of the current study appear to contrast with those of Svec *et al.* (2016), which observed significantly greater GN disruption for 10 OSNHL participants than for 9 YNH participants for a masker-signal delay of 75 ms, a finding that was not replicated here. Instead, GN

disruption was similar for all three participant groups for the 75- and 150-ms masker-signal delays. Svec and colleagues argued that persistence of listener uncertainty between the narrowband masker and sinusoidal target was perhaps greater for the OSNHL than for the YNH participants. Due to the lack of significant differences between groups, the results of the current study do not support the notion of persistence of GN disruption for older listeners with or without SNHL. However, note that in addition to testing for GN disruption at a 75-ms masker-signal delay, Svec and colleagues also tested at 25- and 50-ms masker-signal delays, with significantly larger GN disruption having occurred for the OSNHL than for the YNH participants for the 50-ms masker-signal delay condition. It is possible that differences in persistence of GN disruption may exist between individuals with SNHL and NH for masker-signal delays between 25 and 75 ms.

Assessing listener uncertainty by using a diotic presentation of a masker as a comparison to an entirely monaural stimuli presentation should perhaps give investigators pause. Binaural interactions at the level of the MOC and IC (Park, 1998, 2004) may change the perceptual outcomes for masked thresholds. If, for example, cochlear gain reduction is driven by both contralateral and ipsilateral projections from the MOC, then changes in masked threshold due to the introduction of another stimulus, such as a contralateral masker, may result in a physiological change to cochlear gain. Darrow *et al.* (2006) asserted that neural networks within the lateral superior olive may be responsible for preserving a balance in excitation between the two inputs from each ear. Along this line of reasoning, a change to the input of the contralateral ear may elicit a rebalancing of the output of the two sides of the auditory system. Consequently, the introduction of another contralateral stimulus may not entirely reflect simply a reduction in listener uncertainty but could instead reflect physiological changes.

In addition, investigators have measured other aspects of masking due to temporal envelope fluctuations of the stimuli that may be important to consider as we examine the timing relationships

between maskers and signals. For example, Bonino *et al.* (2013) measured masked thresholds for a pure tone in the presence of a masker train that was composed of temporal bursts of random-frequency broadband noise or a two-tone complex. Participants listened to two conditions, one for which the timing of the signal was consistently presented with a light cue within the anticipated listening interval ("temporally-defined"), or the other for which the timing of the signal was ambiguous ("temporally-uncertain"). When using broadband noise maskers, the temporally-uncertain conditions only increased the mean masked threshold by 2 dB relative to the temporally-defined conditions. However, the same comparison using random-frequency, two-tone complex maskers resulted in a 9 dB increase in mean masked threshold. The results demonstrated that uncertainty of the temporal position of the target relative to the masker may contribute to what investigators consider to be informational masking when measuring masked threshold. By design, the random-frequency, two-tone complex maskers had a less predictable temporal envelope than the broadband noise masker, and the pure tone signal may have been much more easily "confused" with a masker component in this condition. If temporal envelope fluctuations of a masker increase the uncertainty of the temporal position or the level of the target, it is likely that some amount of listener uncertainty is contributing to GN disruption. Consequently, while the computation model supports the notion of differences in OHC gain between maskers contributing to GN disruption, other factors such as listener confusion may additionally contribute.

## D. Inhibition and Envelope Coding at the Inferior Colliculus

Evidence from the computational model does not support the notion that offset-driven inhibition to the IC contributes strongly to GN disruption. When using pure-tone maskers, offset-driven inhibition to the IC has been argued to contribute to growth of masking for a 10-ms masker-signal delay (Salimi *et al.,* 2017). Salimi and colleagues used a similar computation model to the

current study by imposing different time delays for sustained excitatory and inhibitory inputs of the IC, resulting in a physiological implementation of a modulation filter that is sensitive to the envelope fluctuation differences between GN and LFN maskers. However, as indicated by the computational model (see Fig. 8), only approximately 3 dB of GN disruption can be attributed to inhibition for the YNH and ONH participants without the inclusion of the efferent system. In contrast, mean behaviorally measured GN disruption was 8 dB for YNH participants and 18 dB for ONH participants. When the computational model included efferents, GN disruption estimates were in good agreement with behavioral results. Given that GN disruption is observable in the IC of rabbits with normal hearing for simultaneous tone-in-noise stimuli (Fan *et al.,* 2021), mechanisms other than offset-driven inhibition likely contribute to GN disruption. One limitation to the approach taken herein is that variations in cell types or timing delays of inhibition were not examined, despite other cells and time-delay values being physiologically plausible (Kim *et al.,* 2020).

For adults, aging reduces inhibition within the auditory brainstem, with or without the contribution of SNHL (Caspary *et al.,* 2008; Parthasarathy *et al.,* 2019). The effect of a reduction in inhibition on GN disruption is unclear, although reduced inhibition would likely affect the sensitivity to fluctuations in the IC that is modeled by excitatory-inhibitory interactions (Nelson and Carney, 2004). Due to less inhibition of a target following a masker, the reduction in inhibition that is associated with older age should lead to *less* forward masking. Consistent with this notion, less forward masking was observed for the ONH (for the LFN masker) and OSNHL participants (for both maskers). However, the ways in which inhibition would differ for the two masker types and, therefore, strongly contribute to GN disruption remain unclear. As noted above, based on the computational model, only 3 dB of GN disruption was attributable to inhibition.

An alternative possibility to inhibition or changes in MOC efferent feedback is that the reduction in envelope coding within the auditory brainstem associated with age (Frisina and Rajan, 2005; Parthasarathy *et al.,* 2019) caused increased GN disruption for the ONH participants. Considering the higher sensation levels presented to the ONH participants relative to the OSNHL participants in the current study, this degraded envelope encoding associated with older age may have solely been revealed for the ONH participants. Note that the computational model did not address changes in envelope coding associated with age, and thus, the authors cannot currently speak to its contribution to GN disruption.

E. Role of MOC Efferent Feedback

Studies examining the physiological response of MOC efferent feedback on firing rate within the IC provide supporting evidence that changes in rate within the IC may have contributed to GN disruption. Physiologically, the onset of MOC efferent feedback is estimated to be 25 ms (time to maximal reduction in OHC gain: Cooper and Guinan, 2003), which is shorter than the masker duration used herein (400 ms), indicating that the MOC was likely active during the later portion of the maskers. After stimulus onset, persisting effects of OHC gain reduction are estimated to decrease rapidly for the first 40 ms with a gradual decline over the following 80 ms (120 ms total) when measured in humans (Roverud and Strickland, 2010) and animals (Guinan, 2018). While these time courses are well established, OHC gain reduction duration has been measured for as long as 75 seconds (Cooper and Guinan, 2003). Roverud and Strickland (2010) varied the duration of a precursor and the delay between the offset of the precursor and the onset of an on-frequency masker while measuring forward- masked thresholds for a brief (6 ms) 4000-Hz pure-tone target. Behavioral results for adults with NH suggested that, for relatively long precursor durations (50-100 ms), on-frequency cochlear gain reduction of 10-20 dB was observed.

For two of the five participants, cochlear gain reduction (4 – 8 dB) was still observed for a precursor-signal delay of 120 ms. These results from Roverud and Strickland provide indirect evidence that reduction in OHC gain associated with the efferent system could have contributed to the GN disruption that was observed for the 25-ms masker-signal delay and, for some participants, up to 150 ms.

Masked-threshold estimates from the computational model suggest there may be an influence of MOC efferent feedback on GN disruption. The computational model suggests that effects of masker type on firing rate within the IC without MOC efferent feedback are insufficient to explain GN disruption for individuals with normal hearing. GN disruption estimated for the computation model without the MOC efferent system was only 3 dB, far less than the mean 8 and 18 dB measured for the YNH and ONH participants, respectively. The addition of MOC efferent feedback to the computational model had the effect of reducing OHC gain within the model, which in turn, caused higher masked thresholds More importantly, the amount of OHC gain reduction varied by masker type. There was a greater reduction in OHC gain for the GN than for the LFN masker. A greater reduction in gain likely occurred for the GN masker because the IC is physiologically more responsive to stimuli with envelope fluctuations than to those without (e.g., Fan *et al.,* 2021), and synapses from the IC are known to contribute toward regulation of OHC gain (Schofield, 2011). As a result, for the YNH group, OHC gain was reduced for the GN masker relative to the LFN masker (see Figs. 2 & 6), and this difference in OHC gain contributed to an additional 3 dB of GN disruption relative to the computational model without MOC efferent feedback.

The computational model with the efferent system indicates that differences in the relative OHC gain over time between the three groups contributed to the differences observed in behavioral GN disruption between groups. For the computational model of YNH, OHC gain initially

decreased and then steadily increased over the duration of both maskers. In contrast, for the computational model of ONH, OHC gain for the GN masker *decreased* over time. Due to a loss of IHC sensitivity and because OHC gain started out at a lower initial value (due to slight hearing threshold elevations), fluctuations within the IC were greater for the computational model for ONH than for YNH. These more robust fluctuations caused OHC gain to *decrease* instead of increase over the duration of the masker. Consequently, a large GN disruption of 18 dB was predicted by the computational model, with 16 dB of the GN disruption attributable to the MOC efferent system. For OSNHL, the changes in OHC gain that occurred over time were largely reduced relative to the other two groups, owing to their SNHL. Consequently, there was less difference in OHC gain between the two masker types, and therefore, only 1 dB of GN disruption is attributable to MOC efferent feedback.

The current study contributes to prior work attempting to relate perception to MOC efferent feedback by evaluating the consistency of masked thresholds obtained with a computational model of the midbrain with MOC efferent feedback to behavioral measures of GN disruption. Such an approach was also used by Jennings *et al.* (2011) to assess its role in overshoot, a phenomenon in which masked thresholds are more elevated near the onset and offset of a masker than when measured near the temporal center of a masker. While the results of the computation model presented herein indicates that modulation filtering, MOC efferent feedback, and IHC saturation provide plausible explanations for GN disruption, other aspects of auditory processing not assessed here could provide alternative explanations. For example, a number of model parameters are available that were not assessed, including variations on the decision variable used to determine threshold, spontaneous rate of the fiber used for the decision variable, and best modulation frequency of the IC. In addition, the computation model used does not capture all aspects of

auditory processing, such as sustained units (Krishna and Semple, 2000) or the loss of auditory neurons associated with age (Makary *et al.,* 2011).

F. Variability in GN Disruption

Across listeners, the range in GN disruption varied from -4 to 40 dB. While variability in GN disruption decreased as the masker-signal delay increased, some listeners continued to experience up to 30 dB of GN disruption (see Fig. 5). Note that variability across listeners in GN disruption has been previously noted (Svec *et al.,* 2015). The source of this variability is unclear. While age and slight hearing loss influenced GN disruption, variability in GN disruption was still high even for the YNH participants—suggesting that factors other than age or hearing loss contributed toward variance in GN disruption across listeners. One source of variability may have been interval-to-interval variability of the masker envelope. The higher variability in threshold for the GN than LFN maskers at the 25- and 75-ms masker-signal delays (see Fig. 4) support this notion. Variability in firing rate associated with the stochastic nature of auditory neurons may have also contributed. Lastly, additional training could potentially reduce the measured GN disruption (Wright and Zhang, 2009) and some listeners might be better at extracting the relevant perceptual cues and this skill could be more generally related to cognition (Sheft *et al.,* 2015).

G. Implications

There are broader implications of this work. First, possibly the computational modeling presented herein could be extended to provide explanations for the inconsistent relationship observed between MOC function and behavioral effects (e.g., Jennings *et al.*, 2009; Wojtczak *et al.*, 2019). Second, GN disruption has also been measured for simultaneous maskers (Dau *et al., 1996*; Kohlrausch *et al.,* 1997). Given that the MOC efferent system has a 25-ms onset time

(Cooper and Guinan, 2003), one might postulate that GN disruption should not be measurable for maskers of short duration. Kohlrausch *et al.* measured masked thresholds for GN and LFN simultaneous maskers with durations between 20 and 500 ms. GN disruption was smallest at 20 ms and then increased as duration increased. This pattern is consistent with the differences in OHC gain observed between the GN and LFN maskers for YNH. Specifically, the difference in OHC gain increased as masker duration increased. Lastly, this work could have implications for the phenomenon of release from modulation masking (Stone *et al.,* 2011, 2012) and hidden hearing loss (Kujawa and Liberman, 2009; Bernstein and Trahiotis, 2018).

## CONCLUSIONS

- GN disruption was significantly greater for ONH than for YNH or OSNHL participants at a masker-signal delay of 25 ms, suggesting that the loss of cochlear compression associated with hearing loss may not markedly influence GN disruption.
- A computational model of auditory processing in the IC with MOC efferent feedback was able to account for GN disruption and was consistent with the greater GN disruption observed for ONH.
- Possible reductions in envelope encoding in the IC associated with older age could account for the larger GN disruption observed for the ONH participants.

Declarations of interest: None.

## AUTHORS CONTRIBUTIONS

MB and AS designed the research; MB performed the research; MB, BM, and AF analyzed the data and carried out computational modeling; MB and AS wrote the paper. All authors reviewed the paper and provided feedback.

ACKNOWLEDGEMENTS

Funding: This work was supported by the Nebraska Tobacco Settlement Biomedical Research Development Fund (MB) and the National Institutes of Health [010813 to LC, AF, & BM].

REFERENCES

American Speech Language Hearing Association. (2005). Guidelines for manual pure-tone threshold audiometry," Rockville, MD.

ANSI (2004). ANSI S3.6-2004, *Specification for audiometers*, (American National Standards Institute, New York).

Bernstein, L. R., and Trahiotis, C. (2018). "Effects of interaural delay, center frequency, and no more than "slight" hearing loss on precision of binaural processing: Empirical data and quantitative modeling," J. Acoust. Soc. Am. 144(1), 292-307.

Bidelman, G. M., Jennings, S. G., and Strickland, E. A. (2015). "PsyAcoustX: A flexible MATLAB(®) package for psychoacoustics research," Front. Psychol. 6, 1498.

Bonino, A. Y., Leibold, L. J., and Buss, E. (2013). "Effect of signal-temporal uncertainty in children and adults: Tone detection in noise or a random-frequency masker," J. Acoust. Soc. Am. 134(6), 4446-4457.

Brennan, M. A., McCreery, R. W., and Jesteadt, W. (2015). "The influence of hearing-aid compression on forward-masked thresholds for adults with hearing loss," J. Acoust. Soc. Am. 138(4), 2589-2597.

Brennan, M., McCreery, R., Kopun, J., Lewis, D., Alexander, J., and Stelmachowicz, P. (2016). "Masking release in children and adults with hearing loss when using amplification," J. Speech Lang. Hear. Res. 59(1), 110-121.Brown, M. C. (2001). "Response adaptation of medial olivocochlear neurons is minimal," J. Neurophysiol. 86(5), 2381-2392.

Bruce, I. C., Sachs, M. B., and Young, E. D. (2003). "An auditory-periphery model of the effects of acoustic trauma on auditory nerve responses," J. Acoust. Soc. Am. 113(1), 369–388.

Buss, E., Hall III, J. W., and Grose, J. H. (2006). "Development and the role of internal noise in detection and discrimination thresholds with narrow band stimuli," J. Acoust. Soc. Am. 120(5), 2777-2788.

Carney, L. H. (2018). "Supra-threshold hearing and fluctuation profiles: Implications for sensorineural and hidden hearing loss," J. Assoc. Res. Otolaryngol. 19(4), 331-352.

Carney, L. H., and McDonough, J. M. (2019). Nonlinear auditory models yield new insights into representations of vowels. Atten. Percept. Psychophys., 81(4), 1034-1046.

Caspary, D. M., Ling, L, Turner, J. G., and Hughes, L. F. (2008). "Inhibitory neurotransmission, plasticity and aging in the mammalian central auditory system," J. Exp. Biol. 211(11), 1781-1791.

Cooper, N. P., and Guinan Jr, J. J. (2003). "Separate mechanical processes underlie fast and slow effects of medial olivocochlear efferent activity," J. Physiol. 548(1), 307-312.

Darrow, K. N., Maison, S. F., and Lieberman, M. C. (2006). "Cochlear efferent feedback balances interaural sensitivity," Nat. Neurosci. 9(12), 1474-1476.

Dau, T., Püschel, D., and Kohlrausch, A. (1996). "A quantitative model of the ''effective'' signal processing in the auditory system. II. Simulations and measurements," J. Acoust. Soc. Am. 99(6), 3623-3631.

Derleth, R. P., Dau, T., and Kollmeier, B. (2001). "Modeling temporal and compressive properties of the normal and impaired auditory system," Hear. Res. 159(1-2), 132-149.

Desloge, J. G., Reed, C. M., Braida, L. D., Perez, Z. D., and Delhorne, L. A. (2011). "Temporal masking functions for listeners with real and simulated hearing loss," J. Acoust. Soc. Am. 130(2), 915-932.

DiGiovanni, J. J., Lynch, E. E., Nagaraj, N. K., and Ries, D. T. (2018). "Dominance of persistence over adaptation in forward masking," Atten. Percept. Psychophys. 80(7), 1863-1869.

Fan, L., Henry, K. S., and Carney, L. H. (2021). "Responses to diotic tone-in-noise stimuli in the inferior colliculus: stimulus envelope and neural fluctuation cues," Hear. Res. 409, 108328.

Farhadi, A., Jennings, S. G., Strickland, E. A., and Carney, L. H. (2021). A closed-loop gain-control feedback model for the medial efferent system of the descending auditory pathway. In *ICASSP 2021-2021 IEEE International Conference on Acoustics, Speech and Signal Processing (ICASSP)*, 291-295.

Faure, P. A., Fremouw, T., Casseday, J. H., and Covey, E. (2003). "Temporal masking reveals properties of sound-evoked inhibition in duration-tuned neurons of the inferior colliculus," J. Neurosci. 23(7), 3052-3065.

Frisina, R. D. and Rajan, R. (2005). "Inferior Colliculus: Aging and Plasticity," in *The Inferior Colliculus* (pp. 559-584). Springer.

Fuchs, P. A., and Lauer, A. M. (2019). "Efferent inhibition of the cochlea," Cold Spring Harb. Perspect. Med. 9(5), a033530.

Füllgrabe, C., Moore, B. C., and Stone, M. A. (2015). "Age-group differences in speech identification despite matched audiometrically normal hearing: contributions from auditory temporal processing and cognition," Front. Aging Neurosci. 6, 347.

Gai, Y. (2016). "ON and OFF inhibition as mechanisms for forward masking in the inferior colliculus: a modeling study," J. Neurophysiol. 115(5), 2485-2500.

Gifford, M. L., and Guinan Jr, J. J. (1983). "Effects of crossed-olivocochlear-bundle stimulation on cat auditory nerve fiber responses to tones," J. Acoust. Soc. 74(1), 115-123.

Glickman, M. E., Rao, S. R., and Schultz, M. R. (2014). "False discovery rate control is a recommended alternative to Bonferroni-type adjustments in health studies," J. Clin. Epidemiol. 67(8), 850–857.

Guinan Jr, J. J. (2018). "Olivocochlear efferents: Their action, effects, measurement and uses, and the impact of the new conception of cochlear mechanical responses," Hear. Res., 362, 38-47.

Hartmann, W. M., and Pumplin, J. (1988). "Noise power fluctuations and the masking of sine signals," J. Acoust. Soc. Am. 83(6), 2277-2289.

Ibrahim, R. A., and Bruce, I. C. (2010). "Effects of peripheral tuning on the auditory nerve's representation of speech envelope and temporal fine structure cues," In *The neurophysiological bases of auditory perception* (pp. 429-438). Springer.

Jennings, S. G. (2021). "The role of the medial olivocochlear reflex in psychophysical masking and intensity resolution in humans: A review," J. Neurophysiol. 125(6), 2279-2308.

Jennings, S. G., Heinz, M. G., and Strickland, E. A. (2011). "Evaluating adaptation and olivocochlear efferent feedback as potential explanations of psychophysical overshoot," J. Assoc. Res. Otolaryngol. 12(3), 345-360.

Jennings, S. G., Strickland, E. A., and Heinz, M. G. (2009). "Precursor effects on behavioral estimates of frequency selectivity and gain in forward masking," J. Acoust. Soc. Am. 125(4), 2172-2181.

Jesteadt, W., Bacon, S. P., and Lehman, J. R. (1982). "Forward masking as a function of frequency, masker level, and signal delay," J. Acoust. Soc. Am. 71(4), 950-962.

Johannesen, P. T., Pérez-González, P., and Lopez-Poveda, E. A. (2014). "Across-frequency behavioral estimates of the contribution of inner and outer hair cell dysfunction to individualized audiometric loss," Front Neurosci. 8, 214.

Joris, P., Schreiner, C. E., and Rees, A. (2004). "Neural processing of amplitude-modulated sounds," Physiol. Rev. 84(2), 541-577.

Kim, D. O., Carney, L., and Kuwada, S. (2020). “Amplitude modulation transfer functions reveal opposing populations within both the inferior colliculus and medial geniculate body,” J. Neurophysiol. 124(4), 1198-1215.

Kohlrausch, A., Fassel, R., van der Heijden, M., Kortekaas, R., van de Par, S., Oxenham, A. J., and Puschel, D. (1997). “Detection of tones in low-noise noise: Further evidence for the role of envelope fluctuations,” Acta. Acust. Acust. 83(4), 659-669.

Krishna, B. S., and Semple, M. N. (2000). “Auditory temporal processing: responses to sinusoidally amplitude-modulated tones in the inferior colliculus,” J. Neurophysiol. 84(1), 255-273.

Kujawa, S. G., and Liberman, M. C. (2009). “Adding insult to injury: cochlear nerve degeneration after “temporary” noise-induced hearing loss,” J. Neurosci. 29(45), 14077-14085.

Levitt, H. (1971). “Transformed up-down methods in psychoacoustics,” J. Acoust. Soc. Am. 49(2B), 467-477.

Makary, C. A., Shin, J., Kujawa, S. G., Liberman, M. C., and Merchant, S. N. (2011). “Age-related primary cochlear neuronal degeneration in human temporal bones,” J. Assoc. Res. Otolaryngol. 12(6), 711-717.

Meddis, R., and O’Mard, L. P. (2005). “A computer model of the auditory-nerve response to forward-masking stimuli,” J. Acoust. Soc. Am. 117(6), 3787–3798.

Moore, B. C. J. (1981). “Interactions of masker bandwidth with signal duration and delay in forward masking,” J. Acoust. Soc. Am. 70(1), 62-68.

Moore, B. C., Peters, R. W., and Glasberg, B. R. (1992). “Detection of temporal gaps in sinusoids by elderly subjects with and without hearing loss,” J. Acoust. Soc. Am. 92(4), 1923-1932.

Mulders, W. H. A. M., and Robertson, D. (2000). “Evidence for direct cortical innervation of medial olivocochlear neurones in rats,” Hear. Res. 144(1-2), 65-72.

Neff, D. L. (1986). “Confusion effects with sinusoidal and narrowband noise forward maskers,” J. Acoust. Soc. Am. 79(5), 1519–1529.

Nelson, P. C., and Carney, L. H. (2004). “A phenomenological model of peripheral and central neural responses to amplitude-modulated tones,” J. Acoust. Soc. Am. 116 (4 Pt 1), 2173-2186.

Nelson, P. C., Smith, Z. M., and Young, E. D. (2009). “Wide-dynamic-range forward suppression in marmoset inferior colliculus neurons is generated centrally and accounts for perceptual masking,” J. Neurosci. 29(8), 2553-2562.

Nelson, P. C. and Young, E. D. (2010). "Neural correlates of context-dependent perceptual enhancement in the inferior colliculus," J. Neurosci. 19, 6577-6587.

Oxenham, A. J. (2001). “Forward masking: Adaptation or integration?” J. Acoust. Soc. Am. 109(2), 732-741.

Oxenham, A. J., and Moore, B. C. J. (1997). “Modeling the effects of peripheral nonlinearity in normal and impaired hearing,’’ in W. Jesteadt (Eds.), *Modeling sensorineural hearing loss* (pp. 273-288). Lawrence Erlbaum Associates.

Park, T. J. (1998). “IID sensitivity differs between two principal centers in the interaural intensity difference pathway: the LSO and the IC,” J. Neurophysiol. 79(5), 2416-2431.

Park, T. J., Klug, A., Holinstat, M., and Grothe, B. (2004). “Interaural level difference processing in the lateral superior olive and the inferior colliculus,” J. Neurophysiol. 92(1), 289-301.

Parthasarathy, A., Bartlett, E. L., and Kujawa, S. G. (2019). “Age-related changes in neural coding of envelope cues: Peripheral declines and central compensation,” Neurosci. 407, 21–31.

Plack, C. J., Drga, V., and Lopez-Poveda, E. A. (2004). “Inferred basilar-membrane response functions for listeners with mild to moderate sensorineural hearing loss,” J. Acoust. Soc. 115(4), 1684–1695.

Pumplin, J. (1985). “Low-noise noise,” J. Acoust. Soc. Am. *78*(1), 100–104.

Rabbitt, R. D., and Brownell, W. E. (2011). “Efferent modulation of hair cell function,” Curr. Opin. Otolaryngol. Head Neck Surg. 19(5), 376-381.

Roverud, E., and Strickland, E. A. (2010). “The time course of cochlear gain reduction measured using a more efficient psychophysical technique,” J. Acoust. Soc. Am. 128(3), 1203-1214.

Salimi N., Zilany M. S., and Carney L. H. (2017). “Modeling responses in the superior paraolivary nucleus: Implications for forward masking in the Inferior Colliculus,” J. Assoc. Res. Otolaryngol. 18(3), 441-456.

Savel, S., and Bacon, S. P. (2003). “Effectiveness of narrow-band versus tonal off-frequency maskers,” J. Acoust. Soc. Am. 114(1), 380-385.

Schofield, B. R. (2011). Central descending auditory pathways. In Auditory and vestibular efferents (pp. 261-290). Springer, New York, NY.

Sharf, B., Magnan, J., and Chays, A. (1997). “On the role of the olivocochlear bundle in hearing: 16 cases study,” Hear Res. 103, 101-122.

Sheft, S., Shafiro, V., Wang, E., Barnes, L. L., and Shah, R. C. (2015). “Relationship between auditory and cognitive abilities in older adults,” PLoS One. 10(8), e0134330.

Smith, D. W., Turner, D. A., and Henson, M. M. (2000). “Psychophysical correlates of contralateral efferent suppression. I. The role of the medial olivocochlear system in “central masking” in nonhuman primates,” J. Acoust. Soc. 107(2), 933-941.

Stone, M. A., Füllgrabe, C., Mackinnon, R. C., and Moore, B. C. (2011). “The importance for speech intelligibility of random fluctuations in steady background noise,” J. Acoust. Soc. 130(5), 2874-2881.

Stone, M. A., Füllgrabe, C., and Moore, B. C. J. (2012). “Notionally steady background noise acts primarily as a modulation masker of speech,” J. Acoust. Soc. 132(1), 317-326.

Svec, A., Dubno, J. R., and Nelson, P. B. (2015). "Effects of inherent envelope fluctuations in forward maskers for listeners with normal and impaired hearing," J. Acoust. Soc. Am. 137(3), 1336-1343.

Svec, A., Dubno, J. R., and Nelson, P. B. (2016). "Inherent envelope fluctuations in forward maskers: Effects of masker-probe delay for listeners with normal and impaired hearing," J. Acoust. Soc. Am. 139(3), 1195-1203.

Winslow, R. L., and Sachs, M. B. (1988). "Single-tone intensity discrimination based on auditory-nerve rate responses in backgrounds of quiet, noise, and with stimulation of the crossed olivocochlear bundle," Hear. Res. 35(2-3), 165-189.

Wojtczak, M., Klang, A. M., and Torunsky, N. T. (2019). "Exploring the role of medial olivocochlear efferents on the detection of amplitude modulation for tones presented in noise," J. Assoc. Res. Otolaryngol. 20(4), 395-413.

Wojtczak, M. and Oxenham, A. J. (2010). "Recovery from on- and off-frequency forward masking in listeners with normal and impaired hearing," J. Acoust. Soc. Am. 128(1), 247-256.

Wright, B. A., and Zhang, Y. (2009). "A review of the generalization of auditory learning," Philos. Trans. R. Soc. Lond. B. Biol. Sci. 364(1515), 301-311.

Yalçınkaya, F., Yılmaz, S. T., and Muluk, N. B. (2009). "Transient evoked otoacoustic emissions and contralateral suppressions in children with auditory listening problems," Auris, Nasus, Larynx, 37(1), 47–54.

Ye, Y., Machado, D. G., and Kim, D. O. (2000). "Projection of the marginal shell of the anteroventral cochlear nucleus to olivocochlear neurons in the cat," J. Comp. Neurol. 420(1), 127-138.

Zilany, M. S., & Bruce, I. C. (2007). Representation of the vowel /ε/ in normal and impaired auditory nerve fibers: model predictions of responses in cats. J. Acoust. Soc. Am., 122(1), 402-417.

Zilany, M. S. A., Bruce, I. C., Nelson, P. C., and Carney, L. H. (2009). "A phenomenological model of the synapse between the inner hair cell and auditory nerve: Long-term adaptation with power-law dynamics," J. Acoust. Soc. Am. 126(5), 2390–2412.

Zilany, M. S. A., Bruce, I. C., and Carney, L. H. (2014). "Updated parameters and expanded simulation options for a model of the auditory periphery," J. Acoust. Soc. Am. 135(1), 283–286.

Zurek, P. M., and Durlach, N. I. (1987). "Masker-bandwidth dependence in homophasic and antiphasic tone detection," J. Acoust. Soc. Am. 81(2), 459-464.